Metrol. Meas. Syst., Vol. XX (2013), No. 1, pp. 99–106.

PAN POLSKA AKADEMIA NAUK

METROLOGY AND MEASUREMENT SYSTEMS

Index 330930, ISSN 0860-8229

www.metrology.pg.gda.pl

A NEW FORM OF GABOR WIGNER TRANSFORM BY ADAPTIVE THRESHOLDING IN GABOR TRANSFORM AND WIGNER DISTRIBUTION AND THE POWER OF SIGNAL SYNTHESIS TECHNIQUES TO ENHANCE THE STRENGTHS OF GWT

Muhammad Ajab[1], Imtiaz Ahmad Taj[1], Imran Shafi[2], Srdjan Stankovic[3]

1) Muhammad Ali Jinnah University, Department of Electronic Engineering, Kahuta Road, Zone-V, Islamabad, Pakistan (✉ ajabatcop@yahoo.com, +92 332 516 1955, imtiaztaj@jinnah.edu.pk)
2) ABASYN University, Department of Computing and Technology, Plot No. 210, 6, I-9/2, Islamabad, Pakistan (imran.shafi@gmail.com)
3) University of Montenegro, Faculty of Electrical Engineering, Džordža Vašingtona bb, 81 000 Podgorica, Montenegro (srdjan@ac.me)

Abstract

In this paper, a modified form of the Gabor Wigner Transform (GWT) has been proposed. It is based on adaptive thresholding in the Gabor Transform (GT) and Wigner Distribution (WD). The modified GWT combines the advantages of both GT and WD and proves itself as a powerful tool for analyzing multi-component signals. Performance analyses of the proposed distribution are tested on the examples, show high resolution and cross-terms suppression. To exploit the strengths of GWT, the signal synthesis technique is used to extract amplitude varying auto-components of a multi-component signal. The proposed technique improves the readability of GWT and proves advantages of combined effects of these signal processing techniques.

Keywords: Gabor Transform, Wigner Distribution, Gabor Wigner Transform, signal synthesis.

1. Introduction

Time frequency representations (TFRs) are used for non-stationary signal analysis [1–4]. TFRs are generally classified as linear TFRs and quadratic TFRs [2]. The linear TFRs provide cross-terms free representation but with low time-frequency resolution. The time-frequency resolution is improved by using quadratic TFRs. However significant efforts are made to define algorithms for cross-terms suppression, which appear due to the quadratic nature of these distributions [5–7]. In our earlier contribution [7], we have discussed in detail merits and demerits of time representation of a signal, frequency representation of a signal, and the basic goal of a time frequency representation (TFR), linear time frequency representations (TFRs), quadratic TFRs and most widely used cross-term suppression techniques. This contribution [7] also includes a brief discussion on already proposed combination of GWT [8, 9] and exploits the strength of fractional Fourier transform [4–8] to study GWT.

In this paper, a new form of the GWT based on adaptive thresholding of GT and WD has been proposed (Section 2.1). This work has shown that the adaptive thresholding of GT and WD produces the GWT which combines good properties of GT and WD. Numerical examples show that the modified GWT has better resolution comparing to other GWT forms, as well as compared with WD and GT (Section 2.1.1). This work also shows the fusion of signal processing techniques (signal synthesis techniques) and image processing techniques (adaptive thresholding, segmentation and dilation) for cross-terms suppression (Section 3, 3.1). The proposed method is applied to analyze multi-component signal's auto-components extraction and to tackle the resolution problem faced by linear TFRs (Section 3.1.1, 3.1.2).

Article history: received on Oct. 24, 2012; accepted on Jan. 21, 2013; available online on Mar. 15, 2013; DOI: 10.2478/mms-2013-0009.

2. Gabor Wigner Transform

The short time Fourier transform (STFT) [2], is the simplest linear time-frequency transform. If the Gaussian window is used, it is called the Gabor transform (GT) [8]. Mathematically, the GT of a signal $x(t)$ can be written as:

$$GT_x\ (t,\omega)=\sqrt{\frac{1}{2\pi}}\int_{-\infty}^{\infty} e^{-(\tau-t)^2/2}e^{-j\omega(\tau-t/2)}x(\tau)d(\tau)\,. \tag{1}$$

The Wigner Distribution (WD) [1, 2] of $x(t)$ is defined as:

$$WD_x(t,\omega)=\int_{-\infty}^{\infty} x(t+\tau/2)x^*(t-\tau/2)e^{-j\omega\tau}d\tau\,. \tag{2}$$

The formation of the GT and WD is termed Gabor Wigner Transform (GWT) [8]. The following forms of the GWT transforms are introduced:

$$GWT_x(t,\omega)=GT_x(t,\omega)WD_x(t,\omega)\,, \tag{3}$$

$$GWT_x(t,\omega)=\min\{|GT_x(t,\omega)|^2,|WD_x(t,\omega)|\}\,, \tag{4}$$

$$GWT_x(t,\omega)=WD_x(t,\omega)\{|GT_x(t,\omega)|>0.25\}\,, \tag{5}$$

$$GWT_x(t,\omega)=GT_x^{2.6}(t,\omega)WD_x^{0.6}(t,\omega)\,. \tag{6}$$

Equations (3) to (6) show that there is no standard form of GWT and the appropriate choice of GT and WD is crucial for obtaining an optimal resultant transform.

2.1. Modified GWT

The proposed GWT can be written in the form of an algorithm based on the following steps:

Step 1. Find $WD_x(t,\omega)$ of the signal $x(t)$ and its average value T, where:

$$T=mean\,of\,WD_x(t,\omega)\,. \tag{7}$$

Step 2. Classification of the transformed data into sub-classes $WD_A(t,\omega)$ and $WD_B(t,\omega)$ as:

$$WD_A(t,\omega)\in WD_x(t,\omega)\quad if\quad WD_x(t,\omega)\geq T\,, \tag{8}$$

$$WD_B(t,\omega)\in WD_x(t,\omega)\quad if\quad WD_x(t,\omega)<T\,. \tag{9}$$

Step 3. Find averages of $WD_A(t,\omega)$ and $WD_B(t,\omega)$ and update T [10] using the following relation:

$$T=\frac{\mu_{WD_A(t,\omega)}+\mu_{WD_B(t,\omega)}}{2}\,. \tag{10}$$

This iterative procedure will go on until T does not change in two consecutive iterations.

Step 4. The same steps 1 to 3 will be repeated for GT analysis of the signal $x(t)$.

Step 5. Choose:

$$WD_x(t,\omega)=\begin{cases}0 & \text{if } WD_x(t,\omega)\leq T\\ WD_x(t,\omega) & \text{otherwise}\end{cases} \tag{11}$$

Choose:

$$GT_x(t,\omega) = \begin{cases} 0 & \text{if } GT_x(t,\omega) \le T \\ GT_x(t,\omega) & \text{otherwise} \end{cases} \tag{12}$$

Step 6. Multiply $WD_x(t,\omega)$ and $GT_x(t,\omega)$ obtained in Step 5 as:

$$GWT_x(t,\omega) = GT_x^{0.5}(t,\omega) WD_x(t,\omega). \tag{13}$$

2.1.1. Numerical simulations

We consider the example of a signal consisting of three quadratic components (Fig. 1, the sampling frequency is equal to 200 Hz and the time duration is from –1 to 1 second). As it is well-known, the WD suffers from cross-terms due to its quadratic nature (Fig. 1a). GT shows its linearity with low concentration of auto-terms (Fig.1b). By using different forms of GWT (3–6) the time-frequency representation can be improved (Fig. 1c–f). However, by applying the proposed algorithm, the best time-frequency representation will be achieved (Fig. 1g). Thus, it provides cross-terms elimination as in the GT and high resolution as by using the WD. The same example is tested for moderate to high SNR (> 3dB) cases. The modified GWT outperforms other forms of GWT as shown in Fig. 2. The quality of the modified GWT is tested on the basis of entropy measures and ratio of norms [13, 14]. The proposed algorithm gives a maximum value for ratio of norms and minimum value of entropy as shown in Table 1. Hence the modified GWT shows good energy concentration property as compared to other considered TFRs. Therefore our analysis proves that it combines good properties of both WD and GT.

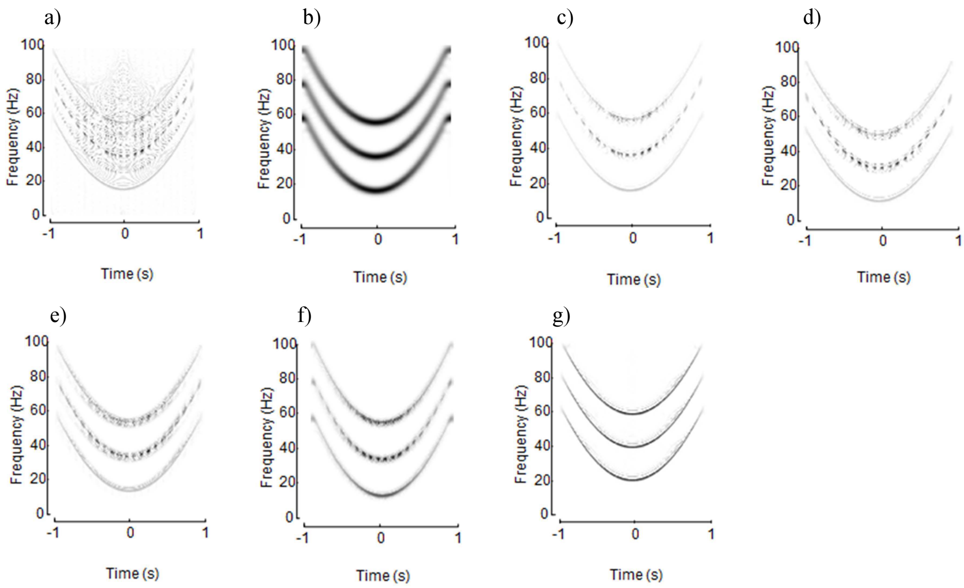

Fig. 1. Three quadratic components: a) WD; b) GT; c) GWT (3); d) GWT (4); e) GWT (5); f) GWT (6); g) Modified GWT.

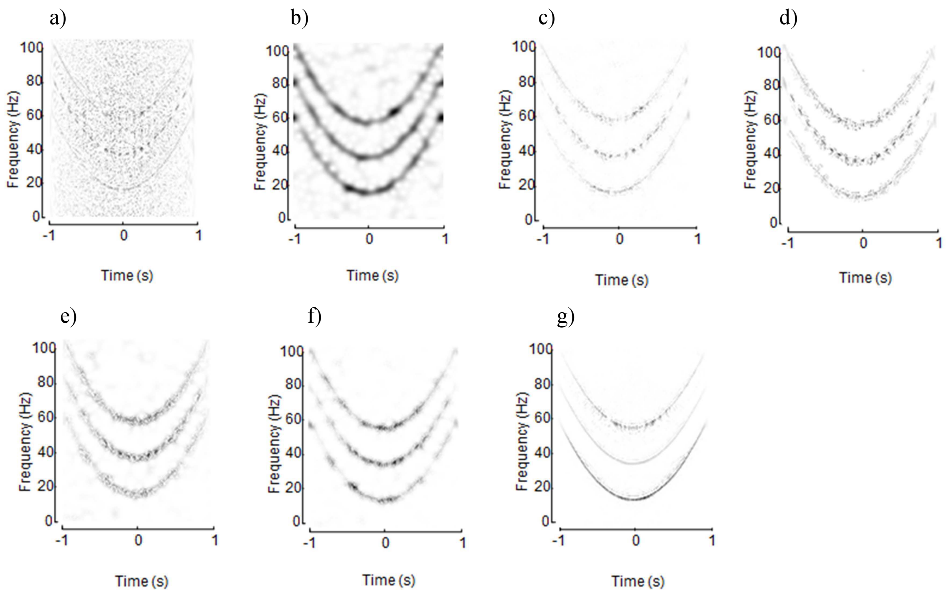

Fig. 2. Three quadratic components (SNR (> 3dB)): a) WD; b) GT; c) GWT (3); d) GWT (4); e) GWT (5); f) GWT (6); g) Modified GWT.

Table 1. Performance measures (Test signal: Three quadratic frequency-modulated components).

TFRs	WD	GT	GWT (3)	GWT (4)	GWT (5)	GWT (6)	Modified GWT
Entropy	16.7041	15.7187	16.1286	14.8550	14.9171	14.8538	**13.2021**
Ratio of norms	0.0251	0.0152	0.1419	0.0599	0.0735	0.1749	**0.2371**

3. Signal synthesis

The signal synthesis technique was proposed in [11]. This technique can be used for time varying filtering and signal separation. In this estimation technique, the signal is generated in such a way that signal's TFR approximates the desired TFR. This method has the following main steps [11, 12]. Suppose $TFR_{x(t)}(t,\omega)$ shows TFR of $x(t)$. The objective is to find out $\hat{x}(t)$ whose $TFR_{\hat{x}(t)}(t,\omega)$ is close to $TFR_{x(t)}(t,\omega)$. To achieve this goal we have to minimize $e(x)$, which is given as:

$$e(x) = \int_{-\infty}^{\infty} \left| TFR_{x(t)}(t,\omega) - TFR_{\hat{x}(t)}(t,\omega) \right| d\omega \,. \tag{14}$$

Equation (14) allows minimization for even ($\hat{x}_e$) and odd ($\hat{x}_o$) samples of $x(t)$. Even (M_{even}) and odd (M_{odd}) matrices elements are given as:

$$M_{even}(i+1, j+1) = g(i+j, i-j) + g^*(i+j, j-i)\,, \tag{15}$$

where: $i, j = 0, \ldots.., L_{even} - 1$

$$M_{odd}(i, j) = g(i+j+1, i-j) + g^*(i+j+1, j-i)\,, \tag{16}$$

where: $i, j = 0, \ldots.., L_{odd}$

In (15) and (16), $g(i, j)$ is the inverse Fourier transform of $TFR_{x(t)}(t,\omega)$, L_{odd} is the length of $\hat{x}_e$ and L_{even} is the length of $\hat{x}_o$.

Phase estimation (φ_e (even) and φ_o (odd)) is described as:

$$\varphi_e = \tan^{-1}\left\{\frac{\mathrm{Re}\left\{\sum_{p=0}^{L_e-1} x(2p)\hat{x}_e^*(p)\right\}}{\mathrm{Im}\left\{\sum_{p=0}^{L_e-1} x(2p)\hat{x}_e^*(p)\right\}}\right\}, \tag{17}$$

$$\varphi_o = \tan^{-1}\left\{\frac{\mathrm{Re}\left\{\sum_{p=0}^{L_o} x(2p-1)\hat{x}_o^*(p)\right\}}{\mathrm{Im}\left\{\sum_{p=0}^{L_o} x(2p-1)\hat{x}_o^*(p)\right\}}\right\}, \tag{18}$$

In (17) and (18), $\hat{x}_e(p)$ and $\hat{x}_o(p)$ are given as:

$$\hat{x}_e(p) = \hat{x}_e(p)e^{j\varphi_e}, \tag{19}$$

$$\hat{x}_o(p) = \hat{x}_0(p)e^{j\varphi_o}. \tag{20}$$

3.1. Algorithm

The objective of this work is to design a TFR which should preserve the quality of auto-components for the multi-component dynamic signals. The steps of the proposed method are given as:

Step 1. Transform the given signal $x(t)$ into GWT by using (3).

Step 2. Adaptive thresholding and image segmentation [7, 10] of the process performed in step 1 and identification of auto-components.

Step 3. Dilation [10] of the process performed in step 2.

Step 4. Time varying filtering [11] by using step 3.

Step 5. Subtraction of estimated auto-component $\hat{x}(t)$ from the original signal $x(t)$.

Step 6. Highly readable TFR is obtained as follows:

$$GWT_x(t,\omega) = GT_x^{0.5}(t,\omega)WD_x(t,\omega), \tag{21}$$

$$TFR_X(t,\omega) = \sum_k GWT_{x_k}(t,\omega), \tag{22}$$

where: k = no of reconstructed auto-components.

The proposed algorithm works in an iterative nature, and normally the number of iterations is equivalent to the number of auto-components. In case of weak auto-components the number of iterations is gradually increased.

3.1.1. Numerical simulation

To show the strength of the proposed algorithm, consider the following example (23).

$$\begin{aligned} x(t) = {} & 0.4\exp(-2\pi j(6t^3 + 50t)) + 0.6\exp(-2\pi j(6t^3 + 30t)) + \\ & 0.8\exp(-2\pi j(6t^3 + 15t)) + 0.7\exp(-2\pi j(75t))\exp(-15t^2), \end{aligned} \tag{23}$$

First auto-components are isolated (Fig. 3a–d). By applying the proposed algorithm step by step, the effect of time-varying filtering is shown in Fig. 3e (cross-terms free TFR). The proposed technique extracts successfully all auto-components and gives a highly readable TFR. This algorithm also proves that the combined effect of signal processing and image processing techniques (Fig. 4d) gives solution of cross-terms of WD (Fig. 4a), blurring faced by GT (Fig. 4b) and low readability and missing component of GWT (3) as shown in Fig. 4c.

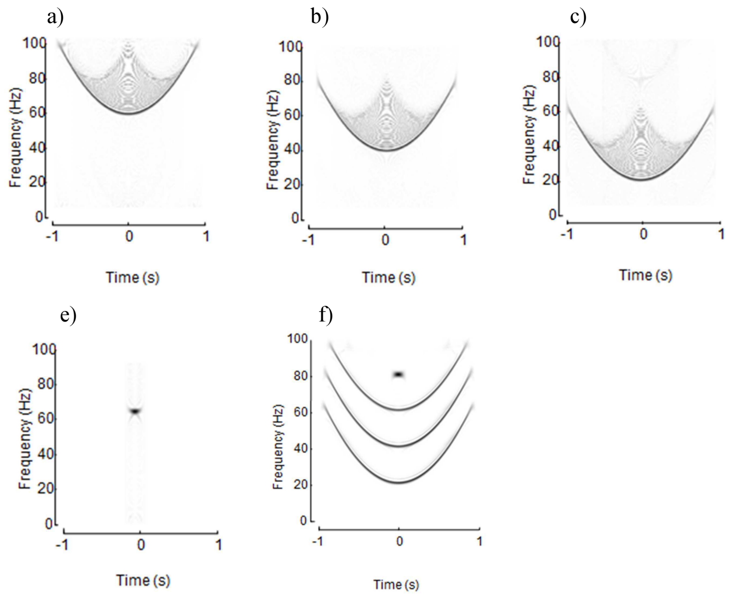

Fig. 3. Three quadratic-components and a Gaussian atom: a) Fist isolated auto-component; b) 2nd isolated auto-component; c) 3rd isolated auto-component; d) 4th isolated auto-component; e) TFR obtained by signal synthesis.

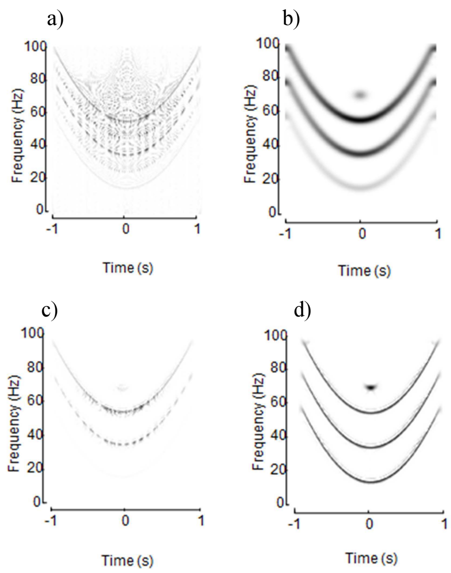

Fig. 4. Three quadratic-components and a Gaussian atom: a) WD; b) GT; c) GWT (1); d) GWT (by using the signal synthesis technique).

3.1.2. Performance analysis

The performance of a TFR is normally evaluated on the basis of ratio of norms, entropy measures and the Ljubisa measure [13–16]. If a TFR has a maximum value of ratio of norms and minimum value of entropy and Ljubisa measure then it is considered as a concentrated and high resolution TFR. The proposed technique has a minimum value of entropy and Ljubisa measure and maximum value for ratio of norms (except modified fractional GWT [7] and Nabeel [6]) as shown in Table 2. Hence the proposed TFR fuses the merits of signal processing techniques and image processing techniques.

Table 2. Performance analysis (Test signal: 3 quadratic-components and a Gaussian atom).

TFRs	Shannon Entropy	Renyi Entropy	Ratio of Norms (× 1.0e–003)	Ljubisa (× 1.0e+009)
WD	16.1481	15.1764	0.0495	1.4116
GT	15.9242	15.0367	0.0532	1.5082
GWT (3)	14.7101	13.9063	0.2066	0.2782
GWT (4)	14.8139	13.8828	0.1355	0.2811
GWT (5)	14.7700	13.4737	0.1871	0.3052
GWT (6)	14.6396	13.3426	0.4077	0.3678
Nabeel [6]	14.2968	13.1015	0.2320	0.2675
Modified Fractional GWT [7]	13.8139	12.3426	0.4663	0.2460
GWT (by using signal synthesis)	**14.3266**	**13.4046**	**0.2163**	**0.2790**

4. Conclusions

This work demonstrates the advantages of the proposed modified GWT in the analysis of time-varying multi-component signals. The proposed combination of GT and WD leads to the resultant GWT, eliminates cross-terms while keeping the resolution of auto-components as in the WD. Moreover, the proposed distribution provides better concentration of auto-components compared with other GWT forms. In this work, GWT's strengths are exploited by using the signal synthesis technique. In our proposed methodology, we have introduced a novel scheme to obtain a high-resolution TFR. The performance analysis of the proposed method reveals it outperforms other TFRs (WD, GT and GWT forms) as described in Table. 2. Hence the proposed TFR fuses the merits of the signal processing technique and image processing techniques. The proposed algorithm can be furnished by applying advanced signal synthesis techniques and image segmentation techniques for the analysis of more complicated signals and to cater low resolution of linear TFRs, which may be a topic of future work.

References

[1] Cohen, L. (1989). Time-frequency distributions-A review. *In Proc. IEEE*, 77, 94–981.

[2] Hlawatch, F., Boudreaux-Bartels, G.F. (1992). Linear and quadratic time frequency signal representations. *IEEE Signal Processing Magazine*, 9(4), 21–67.

[3] Shafi, I., Ahmad, J., Shah, S.I., Kashif, F.M. (2009). Techniques to Obtaian Good Resolution and Concentrated Time-Frequency Distributions: A Review. *EURASIP Journel on Advances in Signal processing*, 2009, art. ID 673539, DOI: 10.1155/2009/673539.

[4] Boashash, B. (2003). *Time-Frequency Signal Analysis and Processing*. Prentice-Hall, Upper Saddle River, NJ, USA.

[5] Qazi, S., Georgakis, A., Stergioulas, L.K., Bahaei, M.S. (2007). Interference suppression in the Wigner distribution using fractional Fourier transformation and signal synthesis. *IEEE Trans. Signal Process.*, 55, 3150–3154.

[6] Khan, N.A., Taj, I.A., Jaffri, N., Ijaz, S. (2011). Cross-term elimination in Wigner distribution based on 2D signal processing techniques. *Signal Proc., advances in Fractional Signals and Systems*, 91(3), 590–599.

[7] Ajab, M., Taj, A.I. , Khan, A.N. (2012). COMPARATIVE ANALYSIS OF VARIANTS OF GWT FOR CROSS-TERMS REDUCTION. *Metrol. Meas. Syst.*, 19(3), 499–508.

[8] Pei, S.C., Ding, J.J. (2007). Relations between Gabor transforms and fractional Fourier transforms and their applications for signal processing. *IEEE Trans. Signal Processing*, 55(10), 4839–4850.

[9] Szmajda, M., Górecki, K., Mroczka, J. (2010). Gabor Transform, SPWVD, Gabor-Wigner Transform and Wavelet Transform – Tools for Power Quality monitoring. *Metrol. Meas. Syst.*, 17(3), 383–396.

[10] Acharya, T., Ray, A. (2005). *Image Processing: Principles and Applications*. Wiley Interscience, Hoboken, NJ.

[11] Boudreaux-Bartels, F.G., Parks, T. (1986). Time-varying filtering and signal estimation using Wigner distribution synthesis techniques. *IEEE Trans. Acoust., Speech, Signal Process.*, ASSP-34(3), 442–451.

[12] Hassnpour, H. (2008). A time-frequency approach for noise reduction. *Digital Signal Processing*, 18, 728–738.

[13] Jones, D., Park, T. (1992). A resolution comparison of several time-frequency representations. *IEEE Trans. Signal Process.*, 40, 413–420.

[14] Williams, W.J., Brown, M., Hero, A. (1991). Uncertainty, information and time frequency distributions. *In SPIE, Advanced Signal Processing Algorithms*, 1556, 144–156.

[15] Shannon, C. E. (1948). A mathematical theory of communication. Part I, *Bell Sys. Tech J.*, 27, 379–423.

[16] Stankovic, Jubisa. (2001). A Measure of Some Time-Frequency Distributions concentration. *Signal Processing*, 81(3), 212–223.